Biochimica et Biophysica Acta 1838 (2014) 388–397

Contents lists available at ScienceDirect

Biochimica et Biophysica Acta

journal homepage: www.elsevier.com/locate/bbamem

Membrane binding and insertion of the predicted transmembrane domain of human scramblase 1

Itziar M.D. Posada, Jon V. Busto, Félix M. Goñi, Alicia Alonso *

Unidad de Biofísica (Centro Mixto CSIC, UPV/EHU) and Departamento de Bioquímica, Universidad del País Vasco, P.O. Box 644, 48080 Bilbao, Spain

ARTICLE INFO

Article history:
Received 31 May 2013
Received in revised form 19 September 2013
Accepted 25 September 2013
Available online 4 October 2013

Keywords:
Scramblase
Transbilayer
PLSCR1
Lipid phases
Transmembrane helix

ABSTRACT

Human phospholipid scramblase 1 (SCR) was originally described as an intrinsic membrane protein catalyzing transbilayer phospholipid transfer in the absence of ATP. More recently, a role as a nuclear transcription factor has been proposed for SCR, either in addition or alternatively to its capacity to facilitate phospholipid flip-flop. Uncertainties exist as well from the structural point of view. A predicted α-helix (aa residues 288–306) located near the C-terminus has been alternatively proposed as a transmembrane domain, or as a protein core structural element. This paper explores the possibilities of the above helical segment as a transmembrane domain. To this aim two peptides were synthesized, one corresponding to the 19 α-helical residues, and one containing both the helix and the subsequent 12-residues constituting the C-end of the protein. The interaction of these peptides with lipid monolayers and bilayers was tested with Langmuir balance surface pressure measurements, proteoliposome reconstitution and analysis, differential scanning calorimetry, tests of bilayer permeability, and fluorescence confocal microscopy. Bilayers of 28 different lipid compositions were examined in which lipid electric charge, bilayer fluidity and lateral heterogeneity (domain formation) were varied. All the results concur in supporting the idea that the 288–306 peptide of SCR becomes membrane inserted in the presence of lipid bilayers. Thus, the data are in agreement with the possibility of SCR as an integral membrane protein, without rejecting alternative cell locations.

1. Introduction

Cell membranes are composed of an asymmetric lipid bilayer in which proteins are embedded. Some of these proteins, named flippases and floppases, are in charge of maintaining the transbilayer phospholipid asymmetry [1,2], with PS predominantly in the inner leaflet. When cells are challenged, in processes such as blood coagulation or apoptosis, intracellular calcium increases accompanied by PS exposure to the outer leaflet via an ATP-independent pathway [3]. The first described member of the phospholipid scramblase family, human phospholipid scramblase 1 (SCR) seems to be the main protein responsible for this event [4,5]. This multifunctional protein is a type-2 membrane protein of 318 aa. It has been described as a lipid raft-associated protein when multipalmitoylated [6,7]. It has been predicted that SCR contains an N-terminus (1–287 aa) cytoplasmic main portion, a putative transmembrane α-helix (288–306 aa), and a small C-terminus extracellular coil (307–318 aa) [8]. Protein-, lipid- and DNA-binding networks connected to SCR are abundant, since posttranslational acylation acts as a switch controlling the scramblase localization. In the absence of acylation, scramblase 1 is imported into the nucleus where it binds DNA and acts as a transcription factor [9,10].

The nature of the physiological activity of SCR in the cell remains controversial. Its role as a scramblase has been challenged due to its involvement in seemingly unrelated events in cell signaling [9,10]. Also relevant in this discussion is the recent identification of TMEM16F as the responsible protein for the defective phospholipid scrambling in Scott syndrome when truncated [11]. The situation is not better understood from the structural point of view. Sahu et al. [12] found that the EF hand-like calcium-binding domains of the scramblase family showed a marked deviation from the classical sequence, and suggested a novel class of low affinity calcium-binding domains. The scramblase anchoring to the membrane has also been challenged [13] due to high similarities in the sequence with the crystallized homologous At5g01750 from *Arabidopsis thaliana* and also with Tubby-like proteins, presuming that the highly hydrophobic α-helical domain, sometimes considered as a transmembrane domain, might remain buried in the protein core with the palmitoyl residues as the only tether to the bilayer. However, in a recent paper, Francis et al. [14] have provided evidence, based on fluorescence quenching studies, that the C-terminal α-helix inserts into membranes.

Abbreviations: ANTS, 8-aminonaphtalene-1,3,6-trisulfonic acid sodium salt; DID, 1,1′-dioctadecyl-3,3,3′,3′-tetramethyl-indodicarbocyanine; DPX, p-xylene-bis(pyridinium) bromide; GUVs, giant unilamellar vesicles; HFIP, 1,1,1,3,3,3-hexafluoro-2-propanol; LUVs, large unilamellar vesicles; MLVs, multilamellar vesicles; PC, phosphatidylcholine; PE, phosphatidylethanolamine; PG, phosphatidylglycerol; PI, phosphatidylinositol; PS, phosphatidylserine; pSM, palmitoyl sphingomyelin; SCR, human phospholipid scramblase 1, or hPLSCR1; TM, transmembrane; TM19, SCR 288–306 peptide; TM31C, SCR 288–318 peptide

* Corresponding author.
E-mail address: alicia.alonso@ehu.es (A. Alonso).

0005-2736/$ – see front matter © 2013 Elsevier B.V. All rights reserved.
http://dx.doi.org/10.1016/j.bbamem.2013.09.018

In order to shed some light on the SCR interaction with membranes two peptides were synthesized, one consisting of the putative transmembrane domain, TM19 [^{288}KMKAVMIGACFLIDFMFFE^{306}] and a second one containing the TM domain plus the exoplasmic coil, TM31C [^{288}KMKAVMIGACFLIDFMFFESTGSQEQKSGVW^{318}] (Fig. 1). No palmitoylation occurs in this part of the protein under physiological conditions. Using a set of well-established biophysical approaches, we studied the interactions of each peptide with model membranes of differing charges and/or phase structures. The results in this paper, together with published topological predictions, give strong support to the notion that the 288–306 peptide of SCR constitutes a transmembrane domain rather than existing inside the protein core.

2. Materials and methods

2.1. Chemicals

TM31C and TM19 were synthesized and purchased from PolyPeptide Group Laboratories (Strasbourg, France), and stored at −20 °C in powder form. When required, they were dissolved in DMSO (Sigma) or HFIP (Fluka). Egg phosphatidylcholine (PC), spinal cord phosphatidylserine (PS), egg phosphatidylethanolamine (PE), egg phosphatidylglycerol (PG) and liver phosphatidylinositol (PI) were purchased from Lipid Products (Redhill, England). The remaining lipids were all from Avanti Polar Lipids (Birmingham, AL, USA). 8-Aminonaphtalene-1,3,6-trisulfonic acid sodium salt (ANTS), p-xylene-bis(pyridinium) bromide (DPX) and 1,1′-dioctadecyl-3,3,3′,3′-tetramethyl-indodicarbocyanine (DID) were obtained from Invitrogen (Life Technologies, Carlsbad, CA, USA). The polyclonal anti-scramblase antibody was from Oncogene (Cambridge, UK). FITC-linked anti-rabbit antibody was from Abcam (Cambridge, UK) and HRP-linked anti-rabbit antibody was from New England Biolabs (Ipswich, MA, USA). All other reagents were of analytical grade. Assay buffer was 10 mM Hepes, 150 mM NaCl, pH 7.4.

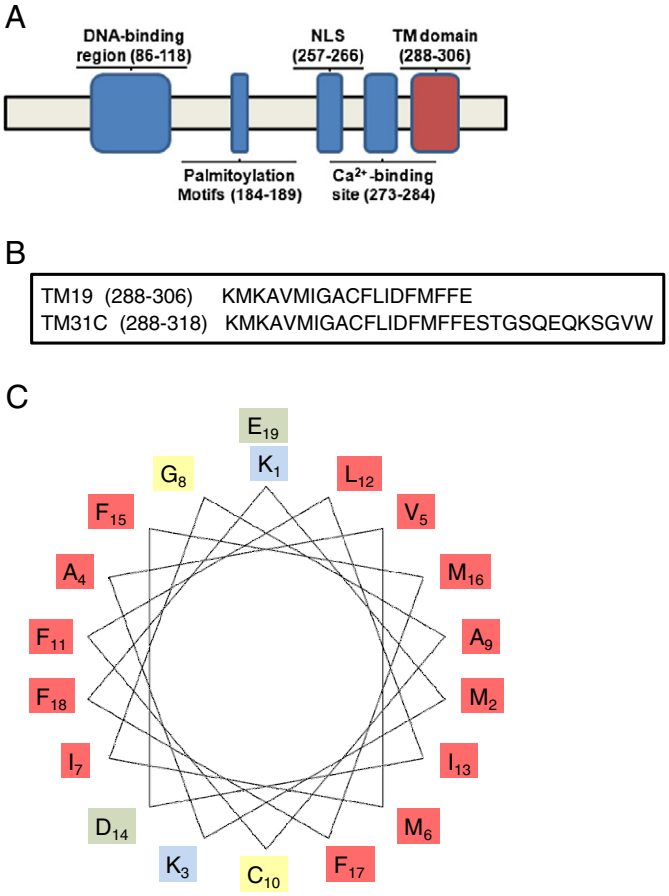

Fig. 1. The structure of human SCR and of the putative transmembrane domain. (A) Human SCR main domains, the predicted transmembrane helix at the C-end is marked in red. (B) The two peptides used in this work, TM19, comprising the transmembrane domain, and TM31C, which includes the TM domain plus the extracellular coil. (C) Wheel diagram of TM19, hydrophobic residues are marked in red.

2.2. Langmuir balance measurements

Peptide-induced changes in surface pressure at the air–water interface and peptide–lipid monolayer interactions were studied at 25 °C using a 1.25 ml multi-well Delta Pi-4 Langmuir balance (Kibron Inc., Helsinki, Finland). Monolayers were formed by spreading a small amount of the lipid mixtures in chloroform:methanol (2:1, v/v) solution on top of assay buffer until the desired initial surface pressure was attained. The peptides dissolved in DMSO (less than 0.5% of total volume) were injected with a micropipette through a hole connected to the subphase, and their surface activity followed by means of surface pressure changes with constant stirring.

2.3. Peptide binding quantification

The appropriate amounts of peptide and LUVs were co-incubated at a lipid-to-peptide ratio 75:1 for 2 h at 25 °C in a ThermoMixer (Eppendorf, Hamburg, Germany). Sucrose gradient formation and ultracentrifugation were carried out as in [15]. A fraction of this sample was adjusted to a 1.4 M final sucrose concentration (final volume 300 μl), overlaid with 400 μl 0.8 M sucrose in buffer, and 300 μl 0.5 M sucrose. The gradient was centrifuged at 400,000 ×*g* for 3 h, and then four 250 μl fractions were collected from the bottom of the tube with a Hamilton syringe. The polycarbonate centrifuge tubes were then washed with 250 μl hot 1% (w/v) SDS to recover the peptide that had aggregated or adhered to the tube walls.

Dot blots were performed using a Hybond-C Extra (Amersham Biosciences) membrane. The sucrose gradient-derived samples were spotted onto the membrane and blocked with 5% skim milk for 1 h, followed by 1 h incubation with anti-scramblase antibody (1:400). The blot was washed several times with PBS, pH 7.4, and incubated for 1 h with an HRP-linked anti-rabbit antibody (1:2000). After final washings to eliminate the unbound secondary antibody, the blot was developed on a Curix 60 processor (AGFA, Belgium) using Amersham Hyperfilm ECL (GE Healthcare, UK). The intensity of the sample signal was measured with a GS-800 densitometer (Bio-Rad, Stockholm, Sweden).

2.4. Differential scanning calorimetry

All measurements were performed using a VP-DSC high-sensitivity scanning microcalorimeter (Microcal, Northampton, MA, USA). For peptide–MLV preparation, the proper amounts of lipid in chloroform:methanol (2:1, v/v) and peptide in HFIP were mixed and the solvents evaporated exhaustively. The MLVs were then prepared by slowly hydrating the peptide-containing lipid film with assay buffer at a temperature above the lipid phase transition temperature, continuously stirring with a glass rod and with vigorous vortexing. The samples were then carefully degassed prior to the measurements. Assay buffer was scanned as a background. The scan rate was 45 °C/h. Samples were scanned several times to ensure the reproducibility of the endotherms. Data were analyzed using ORIGIN software provided by MicroCal. Final volume and lipid concentration in the cell were 0.5 ml and 0.5 mM respectively. Lipid concentration was measured as lipid phosphorous using a molybdate reagent.

2.5. Vesicle content efflux measurements

Large unilamellar vesicles (LUVs) were prepared from MLVs in assay buffer in the presence of ANTS and DPX at a 1:3.6 ratio. The MLVs were extruded 10 times through polycarbonate filters 0.1 μm in pore diameter. The lipid suspension was then passed through a Sephadex PD-10 column to discard non-encapsulated dye. Vesicle content efflux or leakage was measured at 23–25 °C in a FluoroMax luminescence spectrometer following ANTS fluorescence after peptide (dissolved in DMSO) addition. ANTS was excited at 355 nm and emission was recovered at 520 nm using a cut-off filter at 475 nm. The initial vesicle suspension was used to set the 0% fluorescence signal while 100% fluorescence was obtained after vesicle lysis by 1 mM Triton X-100 [16,17].

2.6. Solid-phase binding assay

A screening dot blot analysis was performed to assess the lipid affinities of TM31C [18]. Lipids were dissolved in methanol:chloroform: water (2:1:0.8, v/v/v) at 800 μM final concentration and 1 μl was spotted on a Hybond-C Extra membrane and left for 1 h to let the lipid dry. After blocking with 0.75% skim milk in PBS for 1 h the membrane was incubated for an additional hour with TM31C (500 nM final concentration) also in PBS. The membrane was then washed several times, incubated with antibodies and developed as detailed under Peptide binding quantification.

2.7. Peptide binding to electroformed GUVs and antibody tagging

Giant vesicles were prepared using the electroformation method developed by Angelova et al. [19]. Stock lipid solutions (0.3 mM total lipid containing 0.5 mol% DID) were prepared in a chloroform/methanol (2:1, v/v) solution. 6 μl of the lipid stocks were added onto the surface of two platinum (Pt) electrodes located in a PRET-GUV 4 chamber supplied by Industrias Técnicas ITC (Bilbao, Spain), and solvent traces removed by placing the chamber under high vacuum for 1 h. The chamber was then equilibrated at 55 °C for 15 min and the Pt electrodes covered with 400 μl of a 300 mM sucrose solution, previously equilibrated at 55 °C. The Pt electrodes were connected to a generator (TG330 function generator, Thurlby Thandar Instruments, Huntingdon, UK) under AC field conditions (10 Hz, 0.9 V for 2 h, followed by 1 Hz, 0.9 V for 10 min) at 55 °C. Then, generator and water bath were switched off and vesicles left to equilibrate for 30 min. The chamber (Lab-Tek™ II chambered coverglass, Thermo Scientific) was previously incubated with a 2 mg/ml BSA solution for 30 min to avoid vesicle rupture, and extensively washed thereafter with equiosmolar buffer solution.

Vesicles were then collected and 50 μl added to 250 μl of an equiosmolar TM31C peptide solution (final lipid:peptide ratio of 1:1; final peptide concentration of 0.66 μM) and placed into the chamber. Sucrose-containing vesicles sedimented at the bottom of the chamber due to their higher density, which facilitated vesicle stability and observation under the microscope. Incubation was left overnight at room temperature without stirring and in the darkness. Next, the vesicle solutions were carefully washed 4 times with equiosmolar assay buffer solution to remove non-bound peptide, always maintaining a final volume of 300 μl. The vesicles were then incubated with the anti-scramblase antibody (ratio 1:100) for 1 h under the same conditions. After several washings to remove non-vesicle-bound antibody, a secondary, FITC-linked anti-rabbit antibody (ratio 1:500) was added to the chamber wells and incubated for an additional hour. The chamber was finally washed several times to remove unbound secondary antibody.

2.8. Confocal microscopy

The chambered coverglass containing the GUVs was placed on top of an inverted confocal fluorescence microscope (Leica TCSSP5, Leica Microsystems, Wetzlar, Germany). The excitation wavelengths for FITC (tagging the peptide) and DID (tagging the bilayers) were 488 nm and 633 nm respectively. Emission was recovered between 498–545 for FITC and 650–795 for DID. Both equatorial and 3D images were obtained as required, and treated using the Leica Application Suite software (LAS AF, Leica Microsystems).

2.9. Circular dichroism

CD spectra were recorded using a thermally controlled Jasco J-810 circular dichroism spectropolarimeter in a 0.1 cm quartz cell at room temperature. The spectra were recorded from 190 nm to 250 nm, with 1 nm step resolution, 50 nm/min speed and 100 mdeg sensitivity, data being recorded every 0.2 nm. The results of 40 scans were averaged.

Peptides were prepared in solution in 2 mM Hepes buffer, pH 7.4, in the presence or absence of 50% HFIP, or in membrane-mimicking 100 mM SDS micelles. Stock peptide samples dissolved in HFIP or DMSO were lyophilized or desiccated overnight, and then rehydrated at a 30 μM final concentration. Spectra were buffer-corrected, and normalized to mean residue ellipticity ([θ]) using the equation

$$[\theta] = (\varepsilon)/(10 \cdot C \cdot l \cdot n)$$

where θ is the molar ellipticity (degrees square centimeter per decimole), ε is the ellipticity (millidegrees), C is the protein concentration (millimolar), l is the path length (centimeters), and n is the number of peptide bonds.

3. Results

3.1. Langmuir balance measurements

The SCR sequence-derived transmembrane peptides should exhibit a substantial affinity towards lipid-based membranes. In order to test this hypothesis, we initially performed peptide–lipid interaction studies with the use of lipid monolayers in a Langmuir balance. First, the possible surface activity of TM19 and TM31C was assayed. Fig. S1A displays representative time-courses of TM19-induced changes in surface pressure at the air–buffer interface upon injection of increasing peptide concentrations into the subphase. The peptide induces a dose-dependent increase in surface pressure. The TM domain plus the exoplasmic coil (TM31C) shows a similar surface activity. Both TM19 and TM31C give rise to peptide-based monomolecular films that are saturated at comparable surface pressures (~22 mN/m at 3 μM peptide) (Fig. S1B). Thus, both peptides display a tendency to get adsorbed to air–water interfaces, lowering their surface tension, i.e. they are both surface-active, and both exhibit a similar surface activity.

We next tested the possible peptide–lipid interaction upon injection of TM19 or TM31C into the subphase of a lipid–buffer interface. Specifically, monolayers of either PC or a mixture of PC:PG at a 9:1 mol ratio were prepared at $\pi_0 \geq 22$ mN/m, i.e. above the maximum surface pressure of pure peptides at the air–buffer interface. Addition of 3 μM of either TM19 or TM31C causes a clear increase in surface pressure (see TM31C traces in Fig. S1C). This is interpreted in terms of the peptides becoming inserted into the lipid monolayers. By measuring the peptide-induced maximum π increases at various initial surface pressures (Fig. 2A), two major effects can be observed: i) TM31C presents a higher affinity than TM19 for the studied lipid monolayers and ii) both peptides exhibit a stronger interaction in the presence of 10 mol% negatively charged PG. Moreover, TM19 presents a critical surface pressure (π_c or maximum surface pressure beyond which no peptide insertion occurs), of 27.5 mN/m for PC and 30 mN/m for PC:PG 9:1 monolayers. TM31C shows π_c values of 33 and 37 mN/m for PC and PC:PG monolayers respectively. All π_c values are of the order of magnitude of the estimated 30 ± 5 mN/m for cell membrane lateral pressure [20]. Hence, Langmuir balance assays support a favorable interaction of both peptides, particularly TM31C, with lipid monolayers.

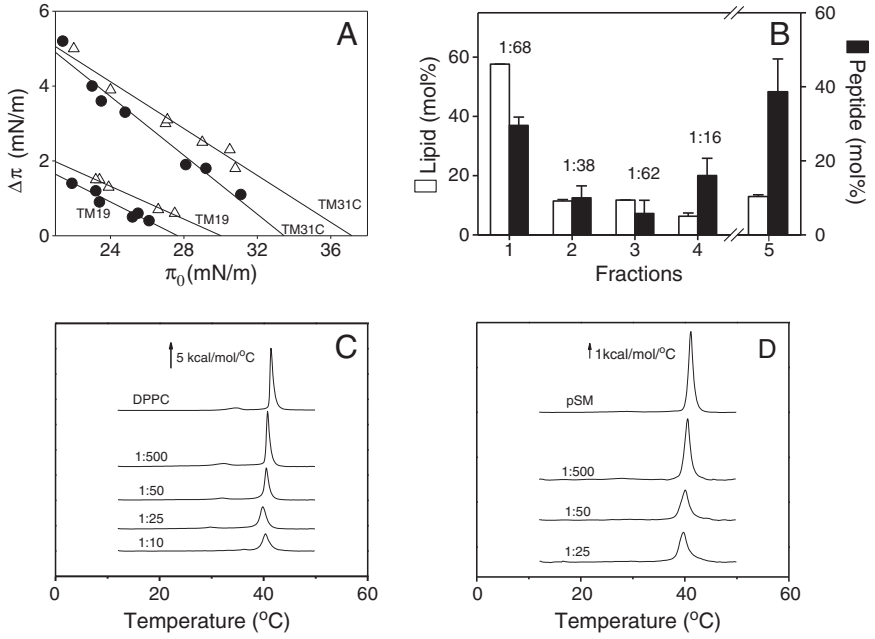

Fig. 2. Peptide interactions with lipid monolayers and bilayers. (A) Insertion of TM31C and TM19 peptides into PC (●) and PC:PG 9:1 (Δ) lipid monolayers. 3 μM peptide was injected into the subphase and monolayers were extended at different initial surface pressures π_0. Equilibrium values of the peptide-induced surface pressure changes are shown. (B) Membrane binding assay of TMC31 peptide by sucrose gradient isolation. 1 to 4, samples recovered from top to bottom of the sucrose gradient. 5 corresponds to the material extracted with 1% SDS from the tube wall. Recovered fractions of lipid (empty bars) and peptide (full bars) are shown. Average values ± SEM (n = 3). Peptide:lipid mol ratios are indicated for each fraction. (C, D) Representative DSC endotherms of pure DPPC (C) or pure pSM (D), and mixtures of those lipids with varying amounts of TM31C (represented as peptide:lipid ratios).

3.2. Membrane binding assays

Peptide interaction with model bilayers was first assessed using a flotation assay, followed by dot blotting and immunodeveloping. TM31C was used together with PC:PG 9:1 bilayers as they presented a higher affinity in monolayer studies. In this assay, after peptide:LUV co-incubation, the sample is layered at the bottom of a sucrose gradient and ultracentrifuged. Liposome-bound peptides float on top of the gradient, whereas the non-bound peptides sediment with the bottom layer.

Fig. S1D displays the dot blot developed for this test and shows that the pure peptide had to be extracted from the tube wall ("P", sample 5). However, the peptide incubated with LUVs remained partly in solution, presumably incorporated into the vesicle membrane in the 4 layers recovered from the tube ("*", samples 1 to 4). Fig. 2B shows the recovered and quantified fractions of lipid and peptide when incubated together; the peptide-to-lipid ratio (mol:mol) is indicated for each fraction. From these results, it can be inferred that when co-incubated, TM31C interacts with PC:PG unilamellar vesicles (about ~60% of the peptide remains bound to LUVs). The most visible band in the gradient is the top one (fraction 1), containing the largest single fractions of both peptide and lipid, at a ≈1:70 mol ratio. This is in accordance with the Langmuir balance studies, however from the binding assays we cannot assess whether the peptide is getting inserted into the bilayer or just adsorbed on the bilayer.

3.3. The effect of TM19 and TM31C on DPPC and pSM bilayers

To further explore the interaction and organization of both peptides in vesicles, we used differential scanning calorimetry (DSC). From the protein or peptide effects on a gel–fluid phase transition of a specific lipid, the kind of interaction, insertion or adsorption, can be inferred [21]. On this basis, we studied mixtures of each peptide with either dipalmitoyl phosphatidylcholine (DPPC) or palmitoyl sphingomyelin (pSM). DPPC and pSM show highly cooperative gel–fluid phase-transitions and are very suitable models for these assays.

Fig. 2C shows the endothermic phase transitions for pure DPPC and mixtures with TM31C. DPPC, as extensively reported, showed a pre-transition at 34 °C and a main phase transition (T_m) centered at 41.3 °C ($\Delta T_{1/2}$ = 0.52 °C and ΔH = 44.6 KJ/mol). Both TM31C and TM19 in the range investigated (from 1:500 to 1:10 peptide:lipid ratio) cause the disappearance of the pre-transition, a clear broadening of the main phase transition and a decrease of the associated enthalpy, while the transition temperature is largely maintained. The abolition of the pre-transition and the decreased enthalpy of the main DPPC phase transition without major changes in T_m are generally associated with insertion processes [21]. Fig. S2B and C show the thermodynamic parameters obtained from the thermograms of DPPC with TM31C and TM19. Both peptides show a similar insertion behavior.

Moreover, interactions of each peptide with palmitoyl sphingomyelin (pSM) bilayers were tested. SM lacks a pre-transition but presents a clear gel–fluid phase transition at similar temperatures as DPPC. Fig. 2D shows the endothermic phase transitions for pure pSM and binary mixtures with TM31C peptide. Pure pSM multilamellar vesicles show a main phase transition centered at 41.1 °C ($\Delta T_{1/2}$ = 0.99 °C and ΔH = 30.9 KJ/mol). In this case peptide addition in the range investigated (from 1:500 to 1:25 peptide:lipid ratio) also caused a significant broadening and loss of the phase transition-related enthalpy as compared to the pure sphingolipid. Fig. S2E and F show the changes on pSM enthalpy and transition width as a function of peptide:pSM ratio for each peptide. In general, the calorimetric data is in good agreement with monolayer studies, showing that both peptides become inserted in phospholipid bilayers.

3.4. Bilayer permeability and solid-phase binding measurements

A series of vesicle content leakage experiments were performed with the aim of studying peptide-induced perturbations in membrane permeability. The following bilayers were used: i) pure POPC in a liquid-disordered (l_d) phase state, ii and iii) egg PC in the presence of 10 mol% negatively-charged PG or PI, iv) PC containing 10 mol%

positively-charged ethylPC, v) a bilayer containing liquid-ordered (l_o) domains, PC:PE:Chol 2:1:1 and vi) PC:oleic acid at a 9:1 ratio.

Fig. 3A shows representative time-courses of TM31C-induced release of ANTS–DPX contents (detected as an increase in ANTS fluorescence upon release from the vesicles) for POPC, PC:PG and PC:PE:Chol. The extent of vesicle efflux is clearly dependent on lipid composition suggesting that peptide insertion is equally sensitive to the lipid mixture in the bilayers.

The steady-state data for the release of ANTS–DPX are shown in Fig. 3B–G for various peptide concentrations. PC:PG (B) induces the maximum observed leakage in the presence of TM31C (around 22%, after ~2 h at R_i 0.02). A lower but still significant content efflux is observed in the presence of any charged lipid, or of oleic acid. Content leakage in the presence of TM31C decreased in the order: PC:PG 9:1 > PC:ethylPC 9:1 > PC:PI 9:1 ≈ PC:oleic acid 9:1 > PC:PE:Chol 2:1:1 > POPC.

TM19 induces a clearly smaller ANTS leakage than TM31C with all tested compositions, probably due to its hydrophobic character and subsequent instability in aqueous solution. Only with PG- and ethylPC-containing vesicles do we observe any substantial content outflow. In general, under any conditions tested, none of our samples behave as the typical lytic peptides, e.g., δ-lysin, or equinatoxin [22–25].

The rates of efflux for the different bilayer compositions could provide some idea of the respective affinities for the peptide. Fig. 4A shows that TM31C causes faster efflux in bilayers containing charged lipids, either PI, ethylPC or PG. Both zwitterionic bilayers show substantially lower rates. The higher efflux from vesicles containing charged lipids can be attributed to the presence of both negatively- and positively-charged residues in the peptides (Fig. 1). Oleic acid-containing bilayers show an intermediate leakage rate. This might be related to a fatty-acid induced decrease in membrane lateral order, thus, a more favorable peptide interaction. A solid-phase binding assay for TM31C and the previous lipid compositions is shown in Fig. 4B. No differences are observed among the assayed mixtures, except for a somewhat lower binding for POPC. Thus, differential binding does not appear to be the main cause for the observed differences in content release and efflux rate probably reflecting a further event beyond binding, i.e. insertion.

3.5. The effect of lipid phase

In order to test the effect of lipid phase and phase segregation on peptide–membrane interactions, we examined TM19- and TM31C-induced vesicle content release in POPC:pSM:Chol mixtures at 22 different ratios selected from the detailed phase diagram by de Almeida and collaborators [26] (Fig. 5A). Fig. 5B shows TM31C-induced representative time-course leakage traces for 7 chosen mixtures at the different regimes. Interestingly, we observe that the mixtures showing higher efflux levels are those presenting a solid-ordered phase (s_o) in coexistence with a l_d, a l_o or both phases. Among these mixtures, the one

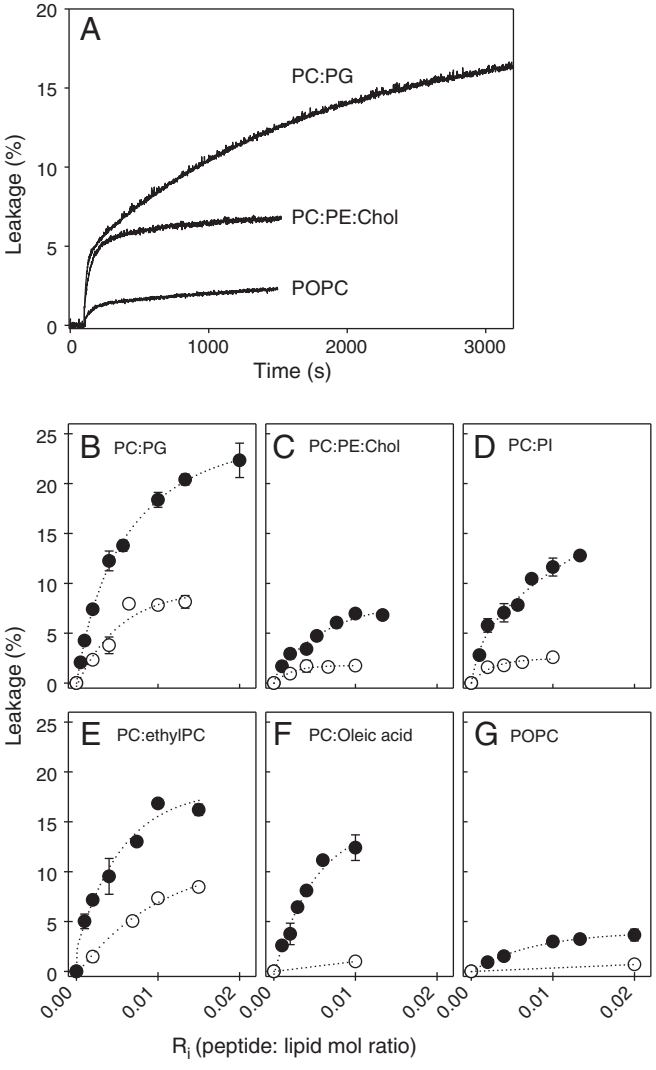

Fig. 3. (A) Representative time-courses of TM31C-induced release of intravesicular aqueous contents for a number of lipid membrane compositions, as indicated for each curve. (B–G) Release of vesicle contents induced by TM19 (○) and TM31C (●) at 25 °C, as a function of peptide:lipid mol ratio. The composition of lipid vesicles (LUV) is (B) PC:PG 9:1, (C) PC:PE:Chol 2:1:1, (D) PC:PI 9:1, (E) PC:ethylPC 9:1, (F) PC:oleic acid 9:1 and (G) POPC. Average values ± SEM (n = 3). Lines are used to guide the eye.

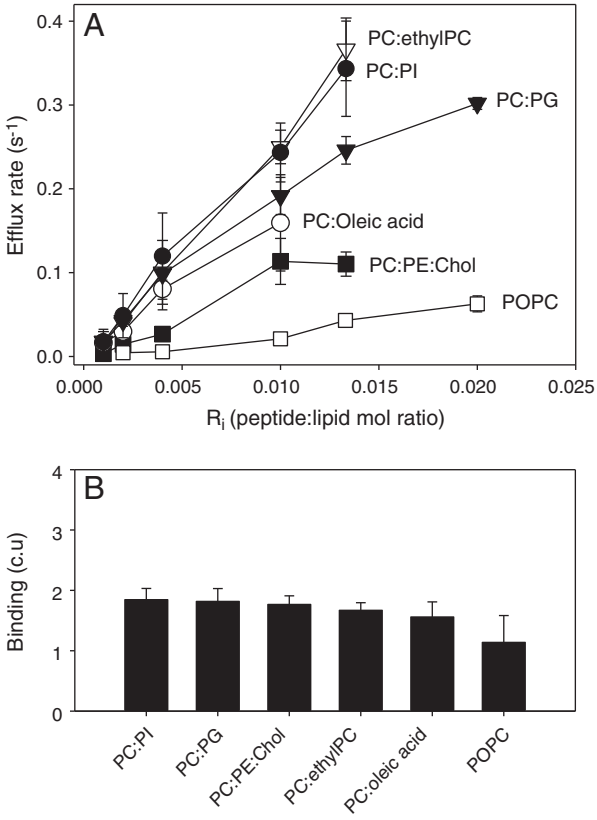

Fig. 4. (A) Slopes derived from time-courses of TM31C-induced leakage, for several vesicle lipid compositions, as a function of the peptide-to-lipid ratio. Average values ± SEM (n = 3). (B) Peptide binding to the same lipid mixtures (c.u., chemiluminescence units).

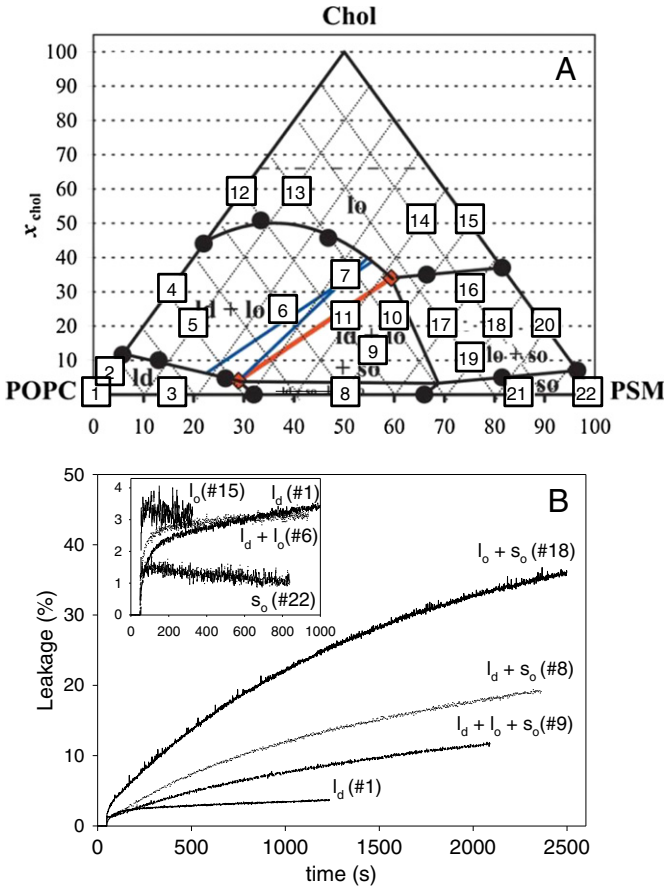

Fig. 5. (A) The 22 lipid mixtures selected from the Almeida et al. POPC:pSM:Chol phase diagram [26] to assay vesicle content release induced by TM19 and TM31C. (B) Time-courses of TM31C-induced leakage of vesicle contents of representative membrane compositions. For each curve the predominant phases and the position in the phase diagram are given. l_d = liquid disordered, l_o = liquid ordered, s_o = solid ordered.

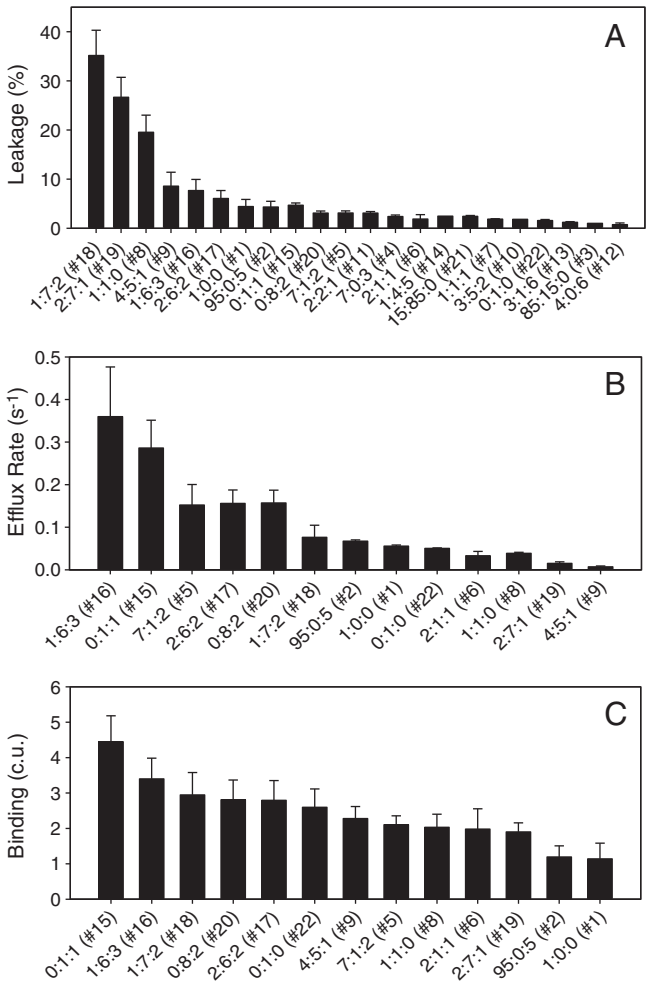

Fig. 6. Membrane binding of TM31C peptide to LUV of different lipid compositions, and subsequent leakage. (A) Extent of release of vesicle contents induced by TM31C. (B) Slopes of selected lipid mixtures. (C) Solid-phase lipid binding assay of TM31C for the same mixtures as in (B). The results are plotted as relative chemiluminescence units for each lipid mixture spotted in the dot blot membrane. Average values ± SEM (n = 3).

containing a l_o–s_o phase coexistence shows the highest efflux. The rest of the vesicles, either made of a pure lipid phase or with phase coexistence in the absence of a s_o phase, causes a lesser membrane perturbation. Vesicles made of pure s_o phase do not present any measurable leakage. In the case of TM19, total release on any of the 22 mixtures tested was less than 3% (data not shown), thus, TM19 data are not discussed any further. From this analysis we conclude that phase segregation could have a direct impact in TM31C-induced vesicle content release. The observed differences between the studied mixtures support an increased peptide–membrane affinity in the presence of certain phase boundaries, the l_o–s_o being the most effective.

Efflux results for the 22 mixtures described in Fig. 5A are presented in full in Fig. 6. Fig. 6A summarizes the extent of TM31C-induced leakage under apparent equilibrium conditions at a 1:50 peptide-to-lipid ratio for the 22 analyzed vesicle compositions. The presence of a s_o phase in the membrane enhances ANTS leakage. This can be clearly noticed in the POPC:pSM:Chol compositions 1:7:2 and 2:7:1 ($l_o + s_o$) or 1:1:0 ($l_d + s_o$). The boundaries between the s_o and the other phases are unstable regions in the membrane, containing structural defects. We propose a more favorable TM31C insertion into the membrane via these boundaries. We can as well notice a larger efflux at 1:7:2 ($l_o + s_o$) vesicle composition in comparison with the 1:1:0 ($l_d + s_o$) vesicles. This could reflect a higher instability of the $l_o + s_o$ boundaries or a preferential affinity of TM31C towards cholesterol-containing interfaces and/or phases.

In Fig. 6B–C, the behavior of TM31C on eleven lipid mixtures among those allowing the highest leakages, is examined in more detail. Fig. 6B reveals an interesting influence of cholesterol on the release rate. The two fastest processes examined occur in mixtures containing 30–50% Chol (mixtures #15, 16), while the slowest releases are found in compositions containing 0–10% Chol (mixtures #8, 9, 19).

Fig. 6C summarizes the results of lipid solid-phase binding assays for the mixtures studied in Fig. 6B. We observe a strong TM31C-binding to 0:1:1 composition (#15) followed by 1:6:3 (#16) composition. POPC:pSM:Chol 1:7:2 composition (#18) that showed high leakage shows also high binding. The presence of cholesterol in the membrane, that enhances leakage rate, also increases the peptide solid-phase binding.

Table 1 summarizes the results obtained from experiments displayed on Fig. 6. There is no strict correlation between peptide binding to bilayers, and rate and extent of content release. However, the combined data appear to indicate that the coexistence of s_o and other phases facilitates the extent of leakage, while cholesterol appears to enhance peptide binding to the membranes, and increase release rates.

The question on whether all mixtures tested would release their aqueous contents through the same mechanism, graded or all-or-none [27], was examined next. The procedure is based on the fact that the lifetimes of calcein fluorescence are concentration-dependent. Analysis of time-resolved fluorescence decay permits the simultaneous observation of different calcein populations. A graded release, as a function of peptide:lipid ratio, should lead to a gradual, peptide-concentration dependent, change in calcein lifetime. Several mixtures were tested but,

Table 1
Membrane binding of TM31C peptide to vesicles (LUV) of different lipid compositions and subsequent permeabilization. Measurements as shown in Figs. 5 and 6. The number in parentheses after the lipid composition refers to the phase diagram in Fig. 5A. Data are average values ± SEM (n = 3).

POPC:pSM:Chol	Leakage (%)	Efflux rate (s^{-1})	Binding (c.u.)
1:0:0 (#1)	4.1 ± 1.03	0.056 ± 0.003	1.1 ± 0.44
95:0:5 (#2)	4.1 ± 1.14	0.068 ± 0.003	1.2 ± 0.32
85:15:0 (#3)	1.4 ± 0.57		
7:0:3 (#4)	2.4 ± 0.31		
7:1:2 (#5)	3.1 ± 0.42	0.153 ± 0.049	2.1 ± 0.25
2:1:1 (#6)	1.4 ± 0.90	0.033 ± 0.010	1.9 ± 0.08
1:1:1 (#7)	1.9 ± 0.07		
1:1:0 (#8)	19.6 ± 3.49	0.038 ± 0.012	2.1 ± 0.37
4:5:1 (#9)	7.9 ± 2.83	0.005 ± 0.002	2.3 ± 0.34
3:5:2 (#10)	1.8 ± 0.15		
2:2:1 (#11)	3.1 ± 0.29		
4:0:6 (#12)	0.5 ± 0.27		
3:1:6 (#13)	1.3 ± 0.60		
1:4:5 (#14)	2.5 ± 0.10		
0:1:1 (#15)	4.6 ± 0.57	0.286 ± 0.065	4.4 ± 0.73
1:6:3 (#16)	7.9 ± 2.25	0.359 ± 0.117	3.4 ± 0.58
2:6:2 (#17)	5.8 ± 1.62	0.156 ± 0.032	2.8 ± 0.56
1:7:2 (#18)	35.5 ± 5.10	0.077 ± 0.028	2.9 ± 0.63
2:7:1 (#19)	28.8 ± 4.04	0.015 ± 0.004	1.9 ± 0.26
0:8:2 (#20)	3.0 ± 0.57	0.157 ± 0.030	2.8 ± 0.56
15:85:0 (#21)	2.4 ± 0.17		
0:1:0 (#22)	1.6 ± 0.20	0.051 ± 0.007	2.6 ± 0.52

as shown in Fig. S4 for three cases, mixtures #1, #8 and #18, allowing very different degrees of leakage, an all-or-none mechanism is clearly observed in all cases, with invariant calcein lifetimes irrespective to peptide–lipid ratios. The all-or-none mechanism also speaks in favor of the efflux being the results of an irreversible insertion, rather than reversible adsorption.

3.6. TM31C location in GUVs

Peptide binding to giant unilamellar vesicles was directly assessed by confocal microscopy. With this aim, vesicles and TM31C were co-incubated and later the peptide tagged with an anti-scramblase C-terminal antibody and a FITC-containing secondary antibody. The confocal micrographs displayed in Fig. 7 correspond to equatorial sections of GUVs electroformed and labeled with the lipophilic probe DID.

Specifically, we addressed TM31C interaction with pure PC, PC:PG (9:1 mol ratio) and POPC:pSM:Chol 1:7:2 (mol ratio). Phase separation in the latter mixture (#18) is clearly seen in the picture, the solid region exhibiting a smaller radius of curvature. Confocal microscopy shows a negligible peptide interaction with pure zwitterionic PC giant vesicles, according to the leakage assay and the solid-phase binding (Figs. 3 and 4). However, direct peptide labeling can be observed in PG-containing vesicles and in the fluid domains of those exhibiting phase separation, as in POPC:pSM:Chol 1:7:2 (mixture #18). The combination of leakage and confocal microscopy would support TM31C insertion into the bilayers and its preferential affinity for negatively-charged and domain-containing bilayers.

3.7. Peptide helicity

The helicity of TM19 and TM31C in solution and in a membrane-mimetic environment was examined using circular dichroism. The results displayed in Fig. S5 show that both TM31C (A–C) and TM19 (B–D) in buffer are unstructured. But upon addition of 50% HFIP or in the presence of membrane-mimicking SDS micelles, TM31C adopts a mainly helical conformation, exhibiting two minima near 208 and 222 nm, characteristic of α-helical conformation. In contrast, TM19 assumes a β structure in both tested cases with a minimum located between 210 and 220 nm, which may indicate TM19 self-association adopting a

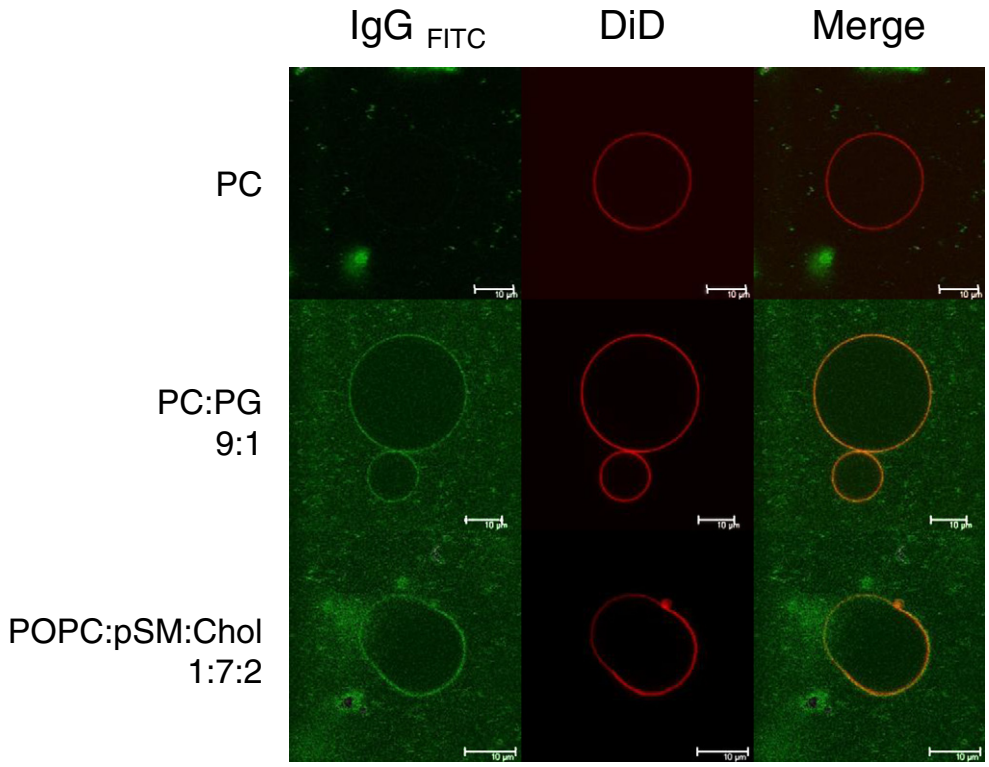

Fig. 7. Imaging of TM31C binding to GUVs. Confocal microscopy of GUVs (equatorial sections) electro-formed from different mixtures of lipids containing 0.5% (mol:mol) DID. Peptide was incubated with vesicles overnight and subsequently incubated with anti-scramblase antibody (1:100) for 1 h. Anti-scramblase antibody was detected by incubating the mixture with FITC 488 goat anti-rabbit IgG (1:500) for an additional hour. Peptide (green) and lipid (red) staining are shown at the left-hand and center columns; the merging of the DID and the FITC images is displayed at the right-hand column.

β-sheet organization. The molar ellipticity of both peptides in HFIP is substantially higher compared to the ellipticity obtained in a micellar environment. The higher propensity of TM31C to form an α-helix may be related to the higher affinity of TM31C for bilayers, as compared to that of TM19, observed in a variety of experiments.

4. Discussion

The results on this paper show that the predicted transmembrane peptide of human SCR is surface active and can insert into lipid monolayers and bilayers in a way that is dependent on the lipid nature and properties. These observations will now be briefly discussed, and put in the context of our current knowledge of SCR.

4.1. The surface properties of TM19 and TM31C peptides

Both peptides under study display surface properties that are potentially interesting in understanding the structure and function of SCR. Specifically:

(i) The peptides are surface active. Both TM31C and TM19 partition at an air–water interface (Fig. S1A–B), demonstrating the surface-active nature of these scramblase regions [28]. An increase in surface pressure in the range of 0.1–1.0 mN/m per residue is to be expected for amphipathic amino acid stretches [29]. In our measurements, the corrected pressure per residue is above 0.77 for both peptides, an indication that almost all the peptide residues are adsorbed to the interface.

(ii) The peptides bind lipid monolayers and bilayers. Both peptides are able to insert into lipid monolayers above the pure peptide-limiting pressure of 22 mN/m as seen in Fig. 2A. The critical pressures or π_c were calculated for each peptide by linear fitting of the experimental $\Delta\pi$ vs. π_0 values and were in both cases of the order of magnitude of the presumed physiological lateral pressure of cell membranes, about 30 mN/m [20]. π_c values were higher for the long peptide, probably due to its stability in solution, and in the presence of the negatively charged lipid PG. These results indicate that scramblase transmembrane domain peptides possess the capacity to interact with monolayers and, as suggested by the π_c values, to insert into bilayers [28,30]. This is in agreement with the recent results by Francis et al. [14]. Moreover, liposomes containing bound peptide are recovered from the top fraction of sucrose gradients after centrifugation (Fig. 2B).
Further evidence for peptide insertion into lipid bilayers arises from DSC. The thermograms obtained for DPPC or pSM in the presence of peptides (Fig. 2C–D and S2A–D) demonstrate their insertion capacity. When a peptide or a protein becomes inserted into a bilayer, the cooperativity of the lipid phase is decreased [21], broadening the transition and lowering the associated enthalpy, as found for cholesterol [31,32]. However, when the peptide or the protein is just adsorbed to the bilayer, lipid cooperativity is not lost and the transition temperature is often increased [33]. The scramblase predicted transmembrane peptides follow the insertion model, with ΔH significantly lowered and the transition peak broadened in all tested cases (Fig. 2C–D and S2). Note that the effects of TM19 and of TM31C on the lipid phase transitions are virtually identical, supporting the notion that the 19-aa stretch reflects a transmembrane domain. The gel–fluid transition of SM appears to be somewhat more responsive to peptide insertion than that of DPPC.
An additional approach to the assessment of peptide–lipid binding is provided by solid-phase binding (Fig. S3, 4B and 6C) [18]. Although this technique does not allow a very precise quantitation, it is useful as a first approximation when a large number of lipids/lipid mixtures have to be tested, as in our case. Moreover, confocal microscopy (Fig. 7) supplies direct evidence of peptide binding to bilayers. Thus, a large variety of techniques and results concurs in demonstrating the membrane affinity of TM19 and TM31C.

(iii) The peptides break the solubility barrier of lipid bilayers. Beyond the mere binding, the peptides cause profound changes in membrane architecture, leading to its permeabilization and subsequent leakage of vesicle aqueous contents (Figs. 3–6 and Table 1). Peptides of multiple origins can permeabilize the lipid bilayer [22–24,34–37]. In our study, in virtually all cases membrane binding was followed by content efflux. These results are discussed in detail below, in the present context they just underline the membranotropic character of our peptides.

4.2. Bilayer permeabilization by TM19 and TM31C

LUV formed from a variety of lipid mixtures was initially tested (Figs. 3 and 4). Peptide binding did not differ greatly with lipid composition (Fig. 4B). The main conclusions were that (i) TM19 was much less effective than TM31C in causing content release, and (ii) electrically charged bilayers, either positively or negatively, supported more extensive and faster release than their zwitterionic counterparts. The low affinity of TM19 in this context is interesting, because the DSC results (Fig. 2 and S2) show that both peptides insert equally well in bilayers. However, for DSC studies lipids and peptides are mixed in organic solvent before bilayer formation, while for content release the peptides are added in a small volume of DMSO to preformed vesicles. The highly hydrophobic nature of TM19 is probably causing its aggregation before it can reach the vesicles, become inserted and cause release, i.e. TM19 activity at the membrane level may be much lower than its total concentration.

The efflux-enhancing role of electric charges in the bilayer is also noticeable (Figs. 3 and 4A), particularly in combination with their lack of effect on membrane binding (Fig. 4B). This probably reflects that binding occurs essentially through hydrophobic interactions, while permeabilization requires the additional concurrence of electrostatic factors. Note that the N- and C-terms of TM19 are charged amino acids, respectively positive (Lys) and negative (Glu). TM31C contains further charged residues that may also help in leakage induction.

4.3. The influence of lipid phases

In zwitterionic bilayers, the presence of saturated and unsaturated phospholipids, and of cholesterol, in different proportions, gives rise to a variety of situations in which different pure phases occur, and often coexist in the same sample, giving rise to domains. A well-studied system of that kind is represented by the POPC, pSM and Chol triangular phase diagram built by de Almeida et al. [26]. A number of mixtures distributed along the phase diagram were selected for our leakage experiments summarized in Figs. 5 and 6, and Table 1. A similar strategy had been followed by Pokorny et al. [22] to study lipid interactions with δ-lysin, a bacterial hemolytic peptide.

Some generalizations can be made in view of the results in Figs. 5 and 6, and Table 1: (i) the extent of leakage is very low for mixtures consisting of pure gel (s_o) phase, e.g., #21 and 22, or for pure l_o phase, e.g., #12 and 13; the opposite is true for mixtures in which the s_o phase coexists with l_d, e.g., #3, or with l_o, e.g., #18 and 19. (ii) There is no strict correlation between mixtures allowing a large extent of efflux and those permitting fast efflux. The fastest rates are found for compositions #15 and 16, rich in pSM and Chol, that supported an intermediate amount of leakage. Mixture #9, in which a coexistence of l_d, l_o and s_o phases occurs, is a slow releaser, but the total efflux is substantial. (iii) The rate of release of vesicular contents is somewhat related to lipid–peptide binding, see e.g., mixtures #15, 16 and 20. (iv) In all cases tested, content release appears to follow an all-or-none mechanism.

The observation that coexisting gel and fluid phases lead to extensive leakage had been done even in pure lipid systems, in the absence of peptides [38–40]. Moreover, some protein toxins have been found that become inserted at the gel–fluid interfaces in bilayers [37]. Pokorny et al. [22] did not observe this interfacial effect, but they did not explore in detail the region of solid–fluid coexistence in the phase diagram. In any case, it should be noted that our peptides, even the most active one TM31C, never achieved above 40% release in our hands, much less than δ-lysin that can induce efflux of 80% dye under certain conditions. This is interpreted in terms of the very different presumed functions of TM31C (protein anchor to the membrane) and δ-lysin (defense peptide). In a recent paper Spaller et al. [41] observe that most peptides that cause all-or-none release are not hemolytic, and the opposite is due of peptides causing gradient release of vesicular contents (note, however, that the hemolytic protein α-hemolysin from *Escherichia coli* did cause all-or-none release of liposomal contents [42]).

4.4. The 288–306 peptide as a transmembrane domain

The main object of this work was to elucidate whether or not the 288–306 peptide of SCR could be a transmembrane domain, hence to test the possibility of SCR as a membrane protein under physiological conditions. The experiments described above provide multiple indications that the 288–306 peptide becomes inserted in lipid bilayers in the manner of integral proteins. The experimental data are also supported by theoretical predictions. According to the Wimley–White octanol hydrophobicity scale [43] the peptide scores negative in free energy ($\Delta G = -1.01 \pm 0.13$), so it is predicted to be transmembrane. In these calculations, intramembrane Asp residue was considered to be electrically neutral [44]. The same result is obtained when the "translocon biological hydrophobicity scale" [45] is used. Moreover α-helical segments buried inside proteins are significantly less hydrophobic than this one, and the hydrophobic amino acids are not all in one continuous sequence as in our case (Fig. 1) [46].

These predictions cannot be taken by themselves as certainties, but the combination of predictive and experimental work provides a very strong evidence that the 288–306 peptide SCR is indeed membrane-inserted, thus, that the protein, even in the absence of acylation, can be membrane-anchored, as required for the phospholipid transbilayer transport activity.

Acknowledgements

The authors are indebted to Dr. W. Wimley for his help in the structural analysis of the peptides. This work was supported in part by grants from the Spanish Ministry of Economy (Grant No. BFU2011-28566 to AA and No. BFU2007-62062 to FMG) and from the Basque Government (Grant Nos. IT 849-13 to FMG and IT 838-13 to AA). IMDP and JVB were PhD students supported by the Basque Government.

Appendix A. Supplementary data

Supplementary data to this article can be found online at http://dx.doi.org/10.1016/j.bbamem.2013.09.018.

References

[1] D.L. Daleke, Regulation of transbilayer plasma membrane phospholipid asymmetry, J. Lipid Res. 44 (2003) 233–242.
[2] F.X. Contreras, L. Sánchez-Magraner, A. Alonso, F.M. Goñi, Transbilayer (flip-flop) lipid motion and lipid scrambling in membranes, FEBS Lett. 584 (9) (2010) 1779–1786(3).
[3] P. Comfurius, P. Williamson, E.F. Smeets, R.A. Schlegel, E.M. Bevers, R.F.A. Zwaal, Reconstitution of phospholipid scramblase activity from human blood platelets, Biochemistry 35 (1996) 7631–7634.
[4] F. Bassé, J.G. Stout, P.J. Sims, T. Wiedmer, Isolation of an erythrocyte membrane protein that mediates calcium transbilayer movement of phospholipids, J. Biol. Chem. 271 (1996) 17205–17210.
[5] Q. Zhou, J. Zhao, J.G. Stout, R.A. Luhm, T. Wiedmer, P.J. Sims, Molecular cloning of phospholipid scramblase 1. A protein mediating transbilayer movement of plasma membrane phospholipids, J. Biol. Chem. 272 (1997) 18240–18244.
[6] J. Sun, M. Nanjundan, L.J. Pike, T. Wiedmer, P.J. Sims, Plasma membrane phospholipid scramblase 1 is enriched in lipid rafts and interacts with the epidermal growth factor receptor, Biochemistry 41 (20) (2002) 6338–6345.
[7] T. Wiedmer, Q. Zhou, M. Nanjunda, P.J. Sims, Palmitoylation of phospholipid scramblase 1 controls its distribution between nucleus and plasma membrane, Biochemistry 42 (2003) 1227–1233.
[8] S.K. Sahu, S.N. Gummadi, N. Manoj, G.K. Aradhyam, Phospholipid scramblases: an overview, Arch. Biochem. Biophys. 462 (1) (2007) 103–114.
[9] I.B. Efraim, Q. Zhou, T. Wiedmer, L. Gerace, P.J. Sims, Phospholipid scramblase is imported into the nucleus by a receptor-mediated pathway and interacts with DNA, Biochemistry 43 (2004) 3518–3526.
[10] Q. Zhou, T. Wiedmer, P.J. Sims, Phospholipid scramblase 1 binds to the promoter region of the inositol 1,4,5-triphosphate receptor type-1 gene to enhance its expression, J. Biol. Chem. 280 (41) (2005) 35062–35068.
[11] J. Suzuki, M. Umeda, P.J. Sims, S. Nagata, Calcium-dependent phospholipid scrambling by TMEM16F, Nature 468 (7325) (2010) 834–838.
[12] S.K. Sahu, G.K. Aradhyam, S.N. Gummadi, Calcium binding studies of peptides of human phospholipid scramblases 1 to 4 suggest that scramblases are a new class of calcium binding proteins in the cell, Biochim. Biophys. Acta 1790 (2009) 1274–1281.
[13] A. Bateman, R.D. Finn, P.J. Sims, T. Wiedmer, A. Biegert, J. Söding, Phospholipid scramblases and Tubby-like proteins belong to a new superfamily of membrane tethered transcription factors, Bioinformatics 25 (2009) 159–162.
[14] V.G. Francis, A.M. Mohammed, G. Aradhyam, S.N. Gummadi, The single C-terminal helix of human phospholipid scramblase 1 is required for membrane insertion and scrambling activity, FEBS J. 280 (12) (2013) 2855–2869.
[15] J.A. Yethon, R.F. Epand, B. Leber, R.M. Epand, W. Andrews, Interaction with a membrane surface triggers a reversible conformational change in Bax normally associated with induction of apoptosis, J. Biol. Chem. 278 (49) (2003) 48935–48941.
[16] H. Ellens, J. Bentz, F.C. Szoka, H^+- and Ca^{2+}-induced fusion and destabilization of liposomes, Biochemistry 24 (1985) 3099–3106.
[17] F.M. Goñi, A.V. Villar, J.L. Nieva, A. Alonso, Interaction of phospholipases C and sphingomyelinase with liposomes, Methods Enzymol. 372 (2003) 3–19.
[18] S. Dowler, G. Kular, D.R. Alessi, Protein lipid overlay assay, Sci. STKE 129 (2002) pl6.
[19] M.I. Angelova, D.S. Dimitrov, Liposome electroformation, Faraday Discuss. Chem. Soc. 81 (1986) 303–311.
[20] D. Marsh, Lateral pressure in membranes, Biochim. Biophys. Acta 1286 (1996) 183–223.
[21] J.C. Gómez-Fernández, F.M. Goñi, D. Bach, C. Restall, D. Chapman, Protein–lipid interactions. A study of (Ca^{2+}–Mg^{2+}) ATPase reconstituted with synthetic phospholipids, FEBS Lett. 98 (2) (1979) 224–228(15).
[22] A. Pokorny, L.E. Yandek, A.I. Elegbede, A. Hinderliter, P.F. Almeida, Temperature and composition dependence of the interaction of delta-lysin with ternary mixtures of sphingomyelin/cholesterol/POPC, Biophys. J. 91 (6) (2006) 2184–2197.
[23] J.M. Caaveiro, A. Molina, J.M. González-Mañas, P. Rodríguez-Palenzuela, F. Garcia-Olmedo, F.M. Goñi, Differential effects of five types of antipathogenic plant peptides on model membranes, FEBS Lett. 410 (2–3) (1997) 338–342.
[24] G. Wiedman, K. Herman, P. Searson, W.C. Wimley, K. Hristova, The electrical response of bilayers to the bee venom toxin melittin: evidence for transient bilayer permeabilization, Biochim. Biophys. Acta 1828 (5) (May 2013) 1357–1364.
[25] Y. Shai, Z. Oren, Diastereoisomers of cytolysins, a novel class of potent antibacterial peptides, J. Biol. Chem. 271 (13) (Mar 29 1996) 7305–7308.
[26] R.F. de Almeida, A. Fedorov, M. Prieto, Sphingomyelin/phosphatidyl-choline/cholesterol phase diagram: boundaries and composition of lipid rafts, Biophys. J. 85 (4) (Oct 2003) 2406–2416.
[27] H. Patel, C. Tscheka, H. Heerklotz, Characterizing vesicle leakage by fluorescence lifetime measurements, Soft Matter 5 (2009) 2849–2851.
[28] R. Maget-Dana, The monolayer technique: a potent tool for studying the interfacial properties of antimicrobial and membrane-lytic peptides and their interactions with lipid membranes, Biochim. Biophys. Acta 1462 (1–2) (1999) 109–140(15).
[29] L. Sánchez-Magraner, A.L. Cortajarena, F.M. Goñi, H. Ostolaza, Membrane insertion of *Escherichia coli* alpha-hemolysin is independent from membrane lysis, J. Biol. Chem. 281 (9) (2006) 5461–5467.
[30] H. Brockman, Lipid monolayers: why use half a membrane to characterize protein–membrane interactions? Curr. Opin. Struct. Biol. 9 (4) (1999) 438–443.
[31] P.L. Chong, D. Choate, Calorimetric studies of the effects of cholesterol on the phase transition of C(18):C(10) phosphatidylcholine, Biophys. J. 55 (3) (1989) 551–556.
[32] P.R. Maulik, G.G. Shipley, Interactions of N-stearoyl sphingomyelin with cholesterol and dipalmitoylphosphatidylcholine in bilayer membranes, Biophys. J. 70 (5) (1996) 2256–2265.
[33] D. Chapman, J. Urbina, Biomembrane phase transitions. Studies of lipid–water systems using differential scanning calorimetry, J. Biol. Chem. 249 (8) (1974) 2512–2521.
[34] H. Ulm, M. Wilmes, Y. Shai, H.G. Sahl, Antimicrobial host defensins — specific antibiotic activities and innate defense modulation, Front. Immunol. 3 (2012) 249.
[35] P. Wadhwani, R.F. Epand, N. Heidenreich, J. Bürck, A.S. Ulrich, R.M. Epand, Membrane-active peptides and the clustering of anionic lipids, Biophys. J. 103 (2) (2012) 265–274.
[36] S. Sánchez-Martínez, V. Madan, L. Carrasco, J.L. Nieva, Membrane-active peptides derived from picornavirus 2B viroporin, Curr. Protein Pept. Sci. 13 (7) (2013) 632–643.
[37] A. Barlic, I. Gutiérrez-Aguirre, J.M. Caaveiro, A. Cruz, M.B. Ruiz-Argüello, J. Pérez-Gil, J.M. González-Mañas, Lipid phase coexistence favors membrane insertion of equinatoxin-II, a pore-forming toxin from *Actinia equina*, J. Biol. Chem. 279 (33) (2004) 34209–34216(13).

[38] D. Papahadjopoulos, K. Jacobson, S. Nir, T. Isac, Phase transitions in phospholipid vesicles. Fluorescence polarization and permeability measurements concerning the effect of temperature and cholesterol, Biochim. Biophys. Acta 311 (1973) 330–340.
[39] E. Corvera, O.G. Mouritsen, M.A. Singer, M.J. Zuckermann, The permeability and the effect of acyl-chain length for phospholipid bilayers containing cholesterol: theory and experiment, Biochim. Biophys. Acta 1107 (1992) 261–270.
[40] S. Clerc, T.E. Thompson, Permeability of dimyristoyl-phosphatidylcholine/dipalmitoylphosphatidylcholine bilayer membranes with coexisting gel and liquid–crystalline phases, Biophys. J. 68 (1995) 2333–2341.
[41] B.L. Spaller, J.M. Trieu, P.J. Almeida, Hemolytic activity of membrane-active peptides correlates with the thermodynamics of binding to 1-palmitoyl-2-oleoyl-sn-glycero-3-phosphocholine bilayers, J. Membr. Biol. 246 (3) (2013) 257–262.
[42] H. Ostolaza, B. Bartolomé, I. Ortiz de Zárate, F. de la Cruz, F.M. Goñi, Release of lipid vesicle contents by the bacterial protein toxin alpha-haemolysin, Biochim. Biophys. Acta 1147 (1) (1993) 81–88(8).
[43] W.C. Wimley, S.H. White, Experimentally determined hydrophobicity scale for proteins at membrane interfaces, Nat. Struct. Biol. 3 (10) (1996) 842–848.
[44] G.A. Petsko, D. Ringe, Protein Structure and Function, New Science Press, 2004. (195 pp.).
[45] T. Hessa, N.M. Meindl-Beinker, A. Bernsel, H. Kim, Y. Sato, M. Lerch-Bader, I. Nilsson, S.H. White, G. von Heijne, Molecular code for transmembrane-helix recognition by the Sec61 translocon, Nature 450 (7172) (2007) 1026–1030.
[46] C. Snider, S. Jayasinghe, K. Hristova, S.H. White, MPEx: a tool for exploring membrane proteins, Protein Sci. 18 (12) (2009) 2624–2628.